Electronic Supplementary Material (ESI) for CrystEngComm

Supporting information

The catanionic surfactant-assisted syntheses of 26-faceted and hexapod-shaped Cu_2O and their electrochemical performances

Wenpei Kang,[a] Fenglin Liu,[a] Yunlan Su,[b] Dujin Wang,[b] and Qiang Shen*[a]

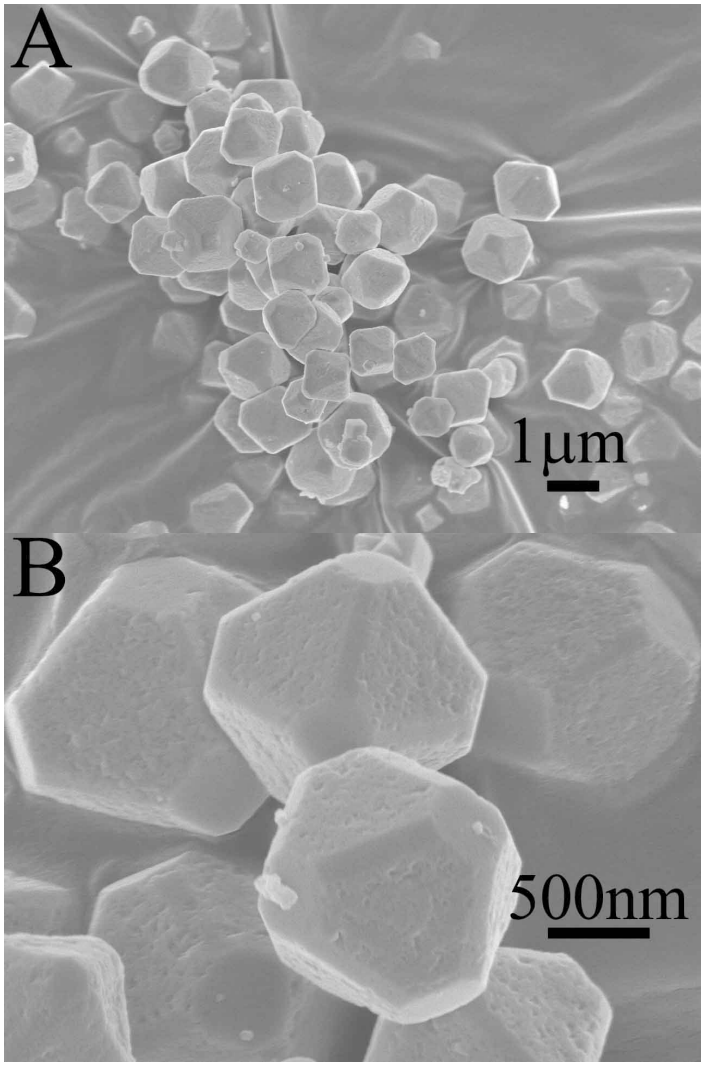

Fig. S2. SEM images of Cu_2O crystalline particles obtained from the anionic-rich catanionic surfactant reaction systems at the SDS/CTAOH molar ratio = 7:5, displaying the 26-faceted polyhedral structure with the relatively small and rectangular {110} faces outside.

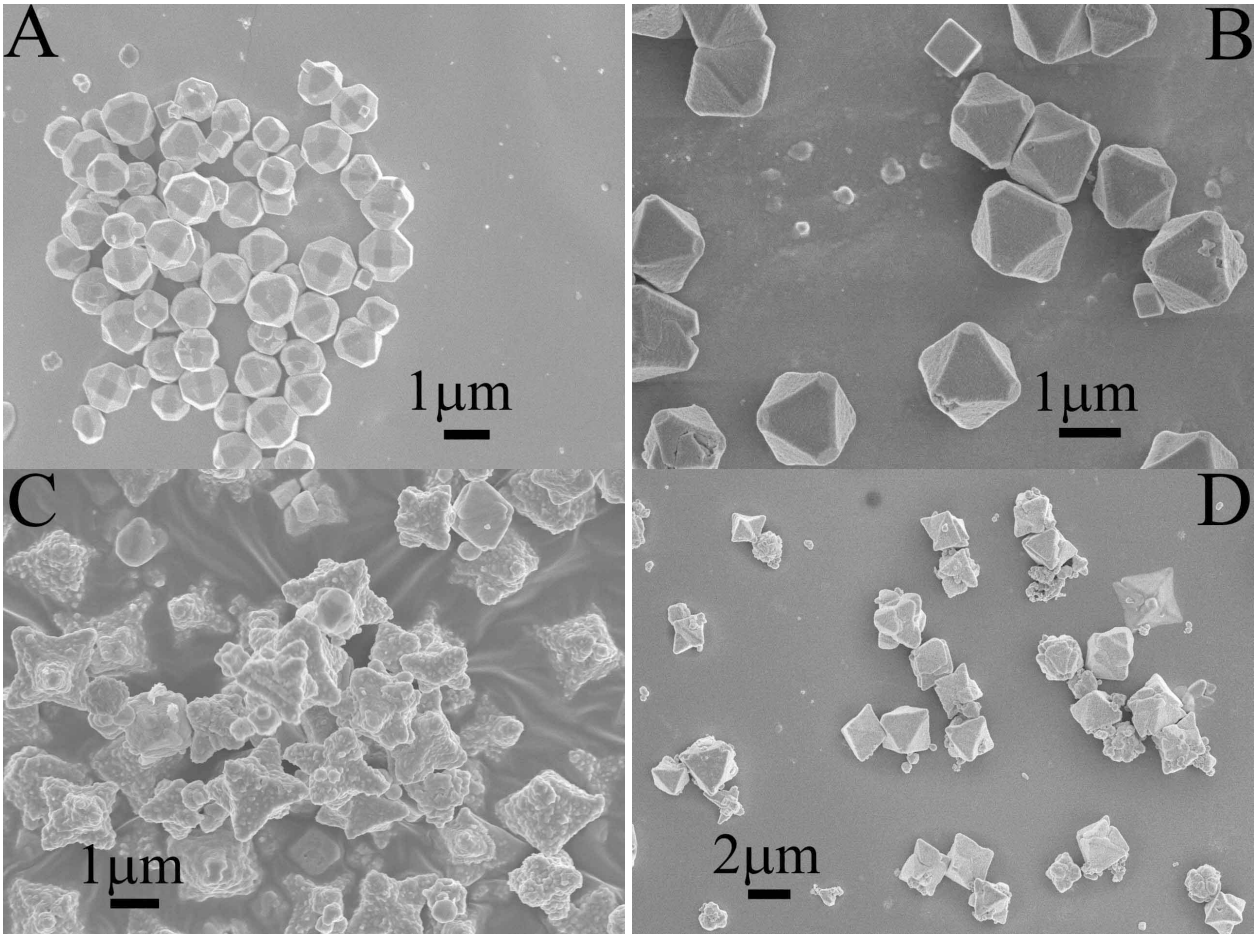

Fig. S2. SEM images of Cu_2O crystalline particles obtained from the anionic-rich catanionic surfactant (SDS/CTAOH molar ratio = 7:4) reaction systems at (A) 60°C and (B) 120°C, and of these sampled from the cationic-rich catanionic surfactant (SDS/CTAOH molar ratio = 4:7) reaction systems at (C) 60°C and (D) 120°C. The 120°C reaction temperature was used to decrease the supersaturation degree and to check the possible formation mechanism of Cu_2O through the secondary nucleation and growth at 60°C, showing the transformation of (A) the 26-faceted crystallites to (B) the truncated octahedrons and of (C) the rough long-hexapods to (D) the smooth short-hexapod-shaped Cu_2O.

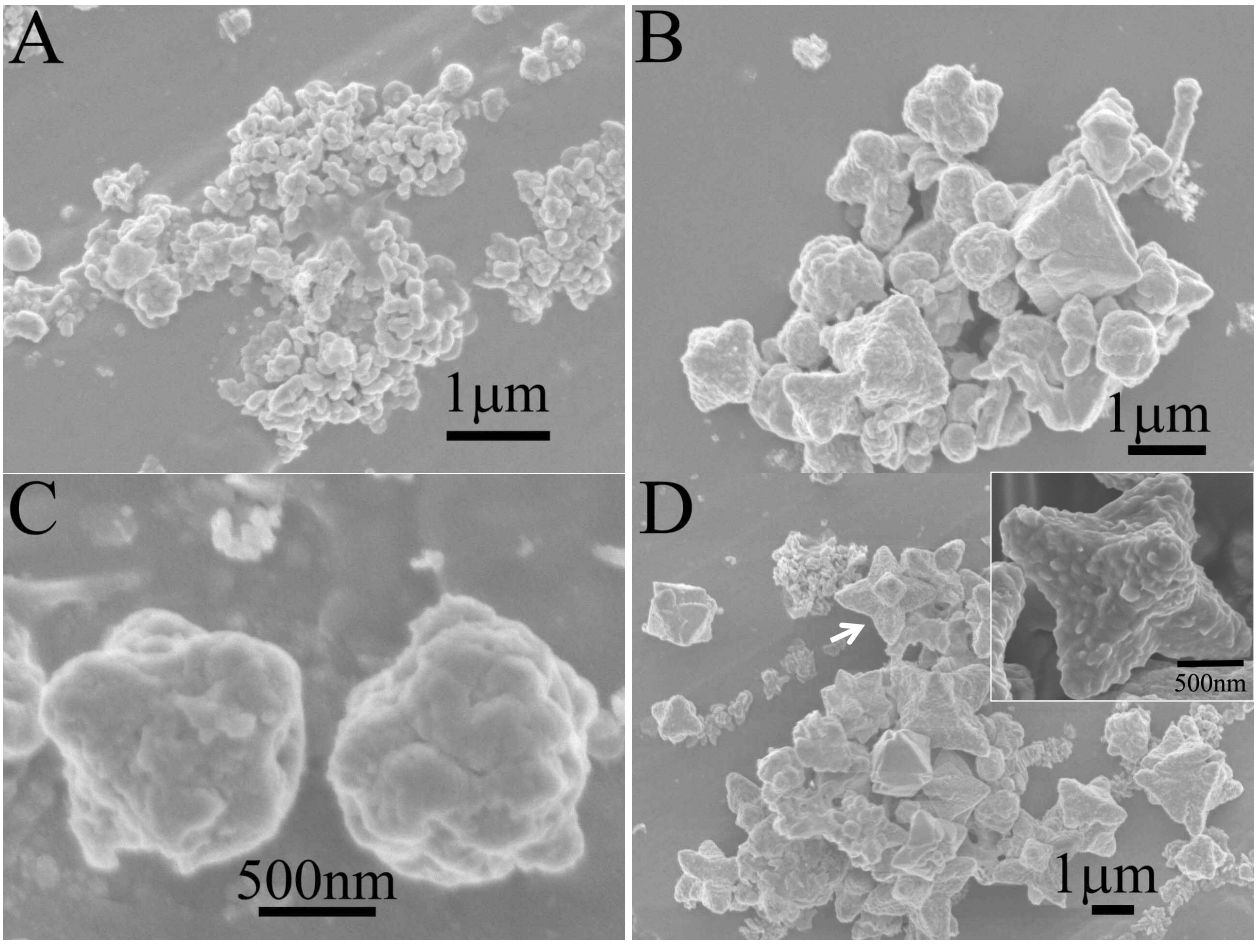

Fig. S3. SEM images of Cu_2O crystalline particles obtained from the cationic-rich catanionic surfactant reaction systems (SDS/CTAOH molar ratio = 4:7, 60°C) at the reaction time of 15 min: (A) the dominant nanoparticles; (B, C) the growing "long-hexapod-shaped" mesoparticles; and (D) the coexistence of tiny nanoparticles, the growing "long-hexapod-shaped" mesoparticles, and the white arrow marked mesoparticles of the grown "long-hexapod". Inset is the representative SEM picture of a grown "long-hexapod-shaped" mesoparticles sampled at the aging time of 48 h. The kinetic (or, the time-dependent) results and the inset indicate that each branch of the primarily formed short-hexapods might grow simultaneously by heterogeneous nucleation with an equal growth rate, otherwise, the grown long-hexapods should experience the unequally colloidal aggregation of tiny nanoparticles onto the symmetrical branches.

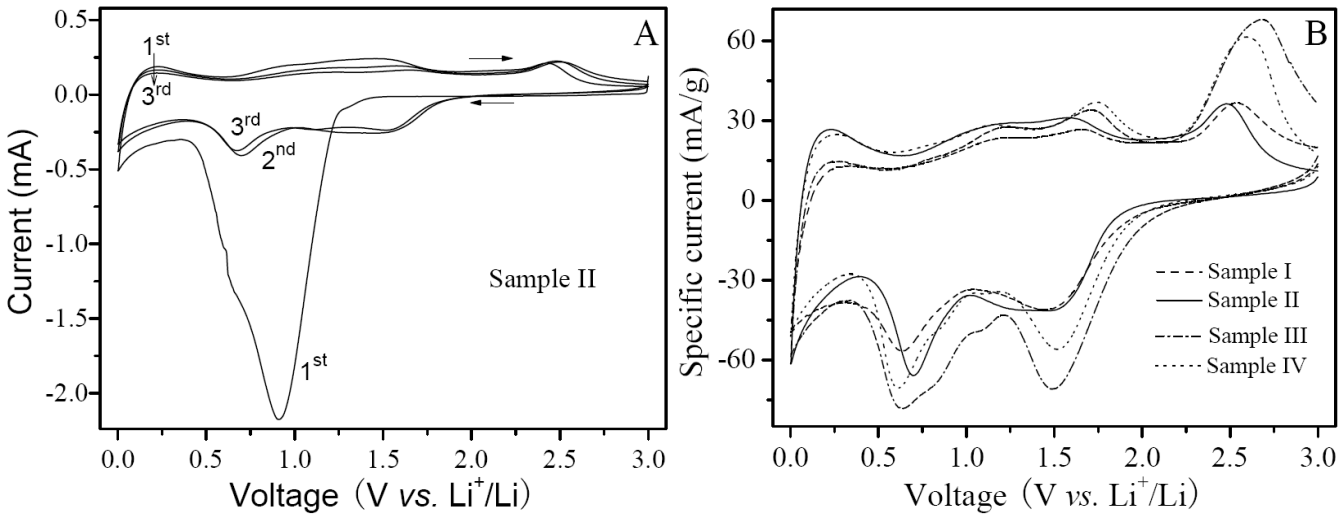

Fig. S4. CV curves of Cu_2O half-cells between 0.0 and 3.0 V at a scanning rate of 0.1 mV/s: (A) the first three cycles for a representative Cu_2O electrode; (B) the second cycles for all of the selected Cu_2O electrodes. In cathodic processes, a broad and intense peak ranging from 1.3 to 0.5 V is observed in the first cycle, then it splits into two cathodic peaks in the range of 2.0 - 1.3 V and 1.0 - 0.5 V during the following cycles (A). For the second cycle therein, the cathodic peak at 2.0 - 1.3 V relates well with the formation of passivation layers of Cu and Li_2O through the reduction of Cu_2O; while the other coincides with the complex side-reactions of electrolyte (i.e., the formation of SEI layers). The peak position of Cu_2O reduction (i.e., the reduction potential) does not change after the first cycle, whereas the peak current of Cu_2O reduction decreases with the cycle number, owing to the formation and consequently thickening of passivation layer. When the weight discrepancies of the active substance in assembled half-cells were taken into consideration, the specific CV peak current of Cu_2O reduction at the second cycle might be used to estimate the thickness of resulting passivation layer therein. Therefore, the thicknesses of passivation layers formed at the second cycling for different Cu_2O shapes are in order: Sample I and/or II > Sample III and/or IV, in reverse proportion to the specific CV peak current of Cu_2O reduction (B).